Article:
Khaemba, DN, Azam, A orcid.org/0000-0002-3510-1333, See, T et al. (2 more authors) (2020) Understanding the role of surface textures in improving the performance of boundary additives, part I: Experimental. Tribology International, 146. 106243. ISSN 0301-679X

https://doi.org/10.1016/j.triboint.2020.106243

Understanding the role of surface textures in improving the performance of boundary additives, Part I: experimental

Doris Nekesa Khaemba[a], Abdullah Azam[b], TianLong See[a], Anne Neville[b], Farnaz Motamen Salehi[b]

[a] The Manufacturing Technology Centre, CV7 9JU, Coventry UK
[b] Institute of Functional Surfaces (IFS), University of Leeds, LS2 9JT

Abstract

Tribological performance of systems in boundary lubrication is dependent on contact and lubricant conditions such as temperature, lubricant additive concentration, surface characteristics, contact pressure and additive-additive interactions. Although past parametric studies have investigated these various factors, there are limited studies on the effect of surface topography on the performance of boundary lubrication additives. This is pertinent because of the increased use of surface texturing in lubricated contacts. This study has employed laser surface texturing to achieve surfaces with different topographies. The influence of the different surface topographies on the tribological performance of a friction modifier additive, molybdenum dialkyldithiocarbamate (MoDTC), was investigated. Results show that laser-textured surfaces in some instances can offer improved friction performance compared to polished surfaces when working positively with a friction modifier additive. Anisotropic surfaces resulted in improved friction. The mechanism for the improved performance of the laser-textured surfaces is believed to be through the augmented local contact pressures at the asperities that accelerate additive decomposition to form protective low-friction tribofilms. This study demonstrates the feasibility of surface texturing in improving the performance of boundary additives.

Keywords

Texture, Boundary, Additives, Friction

1 Introduction

Lubricants are used in many engineering applications to reduce friction and wear and in so doing they improve the efficiency of the systems. Lubricants can provide management for friction and wear primarily because of the presence of various additives in the oils. In engine lubricants, boundary additives such as antiwear additives and friction modifiers are particularly important as they directly influence engine durability and fuel economy [1,2]. These additives perform their various functions through the formation of thin protective films (tribofilms) via tribochemical reactions. As engine lubricants contain boundary additives, significant research has focused on understanding the additive behaviour within contacts (i.e. additive decomposition, tribofilm formation, tribofilm durability). An in-depth understanding of additive behaviour is crucial for product performance optimisation and new product development. In literature, studies have investigated the influence of parameters such as contact pressure, sliding speed, sliding-rolling ratio, temperature, surface roughness, additive concentration and additive-additive interaction [3–10]. Of these parameters, surface topography is of particular interest in many application areas. This is because the tribological performance of components can be improved without requiring changes to the original operating conditions of the component.

Surface modification has gained interest recently due to the development of new processing techniques such as laser texturing which are able to generate surface features with great precision and repeatability. The use of surface modification to improve tribological performance has been demonstrated in cutting tools, metal forming tools, mechanical seals and piston-cylinder liners [11–14]. Majority of surface

features reported in the literature are recessed into the surfaces with common geometries such as dimples, grooves and chevrons [15]. Various mechanisms have been proposed to explain improved tribological performance obtained with surface textures. Some researchers propose that the presence of pocket increase the load carrying capabilities resulting in low friction [16–21]. Other researchers propose that the improved performance of textured surfaces over untextured surfaces is due a debris trapping mechanism where the pockets trap wear debris resulting in smooth surfaces which in turn result in lower friction and wear [22–25]. In other studies, it has also been proposed that textured surfaces entrap lubricant within its pockets and providing a constant supply of lubricant to the contact thus reducing friction and wear [26–29]. Additionally, it has been proposed that optimised surface textures can reduce static friction by up to 50% compared to untextured surfaces. It is worth mentioning that surface textures do not always provide improved tribological performance. Studies by Vladescu et al., [30–35] reported that the performance of surface textures was dependent on the lubrication regime of the contact. It was observed that textures that increased lubricant film thickness resulting in lower friction in boundary and mixed regimes increased friction in hydrodynamic lubrication regimes [32].

Few research groups have reported on the tribological performance of surface textures in the boundary lubrication regime. Bonse et al., [36,37] investigated the performance of Laser-Induced Periodic Surface Structures (LIPSS) in steel and titanium. The mentioned researchers reported significant improvements in wear performance on titanium alloy with fully formulated oil while no improvement was observed with paraffin oil. On steel surfaces, LIPSS had no influence in both paraffin oil and engine oil. The authors suggested that the improvement observed in the titanium alloy, when engine oil was used, was due to the additives in the oil interacting well with the surface structures. Bettscheider et al., [38] reported that friction improvement can be achieved in base oil with line-like surface patterns generated using Direct Laser Interference Patterning (DLIP). Rough surfaces generated using traditional methods such as grinding have been reported to provide conducive conditions for additive degradation resulting in friction reduction and improved wear performance [39]. Additionally, rough surfaces with features oriented perpendicular to the sliding direction have been reported to have a better performance that those oriented parallel to the sliding direction [40].

Although, laser texturing at nano- and micro-scale has been shown to improve friction and wear in the boundary lubrication regime in some studies, more studies are needed to develop a fundamental understanding of the influence of surface features on the performance of boundary additives. This study aims to further this understanding by correlating additive performance to surface topography. In this study, laser surface texturing was employed to generate surfaces with micro-scale surface features of varying orientations. The generated surfaces were subjected to tribological performance evaluation using model oils containing molybdenum dialkyldithiocarbamate (MoDTC), a common friction-modifier additive in engine lubricants. In addition to the experimental work, simulation studies were conducted using inputs from the experiment. Combined results from the experimental and simulation studies provided a holistic view of processes that occurred at the contact interface. The presentation of this study is split into two parts, the experimental work is presented in part I while the simulation work is presented in part II of this paper.

2 Experimental

2.1 Sample preparation

Materials used in the tests were cast iron pins and tool steel plates. The cylindrical pins measured 20 mm in height and 6 mm diameter, the contacting surface of the pin was machined to have a radius of curvature of 10 mm. The tool steel plates measured 15 mm x 6 mm x 3 mm. Table 1 details the material properties and surface finish of the samples used.

Table 1. Material properties

Material	Hardness	Young's modulus	Poisson ratio	S_q
Cast iron (pins)	4.5 GPa	134 GPa	0.26	0.046 µm
Tool steel (plates	6.5 GPa	206 GPa	0.29	0.007 µm

The mirror polished steel plates were laser textured using a P400U laser machine from Georg Fisher Machining Solutions. An IPG nano laser with a 1064 nm wavelength was used. The ablation parameters were 0.5 J/cm^2, 750 kHz frequency, 4 ns pulse duration and 1000 mm/s speed. The laser spot size was approximately 50 µm in diameter and the pulse separation distance was 60 µm (0% pulse overlap). Three different textures were generated by varying the hatch distance and the hatching angle as indicated in Table 2. Spot radiation of the surface by the laser causes the surface material to melt. The force of the laser generates a crater and molten material from the crater is ejected and redeposited on the edges where it solidifies to generate asperities. This process for generating surface textures was selected as it allows surface asperities, which are important in boundary regime, to be generated.

The generated laser textured samples were analysed on a Sensofar S mart machine using white light interferometry configuration at 20x magnification. During the analysis, the samples were aligned in the sliding direction used in the tribology tests. The measured raw data was processed by removing the form and applying a Gaussian filter with a cut-off wavelength of 0.08 mm to remove the waviness.

Table 2. Laser processing parameters for the different texture patterns

Texture	Hatch distance	Hatching angle	Number of passes (NOP)
T1	60 µm	0°, 90°	3125
T2	60 µm	0°, 60°, 120°	3093
T3	120 µm	90°	1562

2.2 Tribological tests

Tribological testing was conducted on a reciprocating Biceri tribometer with a pin-on-plate configuration. Cast iron pins were fixed in position while the steel plates were reciprocated. Test conditions for the tribological tests were as follows; 10 mm stroke length, 50 N load and 1 Hz frequency (20 mm/s speed at mid-stroke). Two oils were used in the tests, a group 3 mineral oil (kinetic viscosity at 40°C=19.3 cSt, kinetic viscosity at 100°C=4.2 cSt) and a blend consisting of 0.5 wt% MoDTC in the group 3 mineral oil (0.05 % Mo and 0.05 % S). Hereafter, the mineral oil will be referred to as base oil or BO and the blend as MoDTC. In this study, a low lubricant temperature of 40°C was specifically selected in order to reduce the contribution of thermal effect on MoDTC decomposition. Previous studies have reported that an increase in temperature above 60°C results in friction reduction in MoDTC containing oils [41]. It is thus anticipated that at a temperature of 40°C used in the present study, there is a reduced thermal effect on MoDTC decomposition. This allows the impact of the surface features on the additive degradation process to be highlighted. Prior to the tribological tests, the tribopair samples were cleaned with acetone in an ultrasonic bath for a few minutes. Tests were run for a duration of 1h. All tests were repeated at least twice to check for repeatability. Average friction results of the tests are reported in the results section.

The calculated initial maximum Hertzian contact pressure under the loading conditions was 0.9 GPa with an initial contacting diameter of 320 µm. The minimum film thickness was calculated using the Hamrock-Dawson equation for EHL point contact. In these calculations, a pressure viscosity coefficient of 1.1 x 10^{-8} Pa^{-1} was used. A minimum film thickness of 80 nm was obtained which provided lambda ratios of 1.71, 0.08, 0.08 and 0.04 for polished, T1, T2 and T3, respectively. Based on these calculations, the polished samples are expected to be in an initial mixed lubrication regime while the laser-textured samples are in boundary lubrication regime.

3 Results

3.1 Morphology of laser textured samples

3D images of the surface topography are shown in Figure 1. The corresponding surface profiles along the sliding direction (used in tribological tests) are included. In evaluating the surface topography both height and spatial parameters were considered. For textured surfaces such as the ones used in this study, height parameters are not enough to differentiate surfaces from each other; two surfaces can have similar height parameters despite having different surface features. The height parameters reported are the arithmetic mean height (S_a), root mean square height (S_q), skewness (S_{sk}) and kurtosis (S_{ku}). The arithmetic mean height is the average height above the mean value of the asperities while the root mean square height is the average squared heights above the mean. The skewness value indicates where the bulk of the material lies. Negative S_{ku} values indicate that the bulk of the material lies above the mean line while positive values indicate that bulk of the material lie below the mean line, Kurtosis, S_{ku} describes the sharpness of the profile peaks. $S_{ku} < 3$ indicates a blunt profile. $S_{ku} = 3$ indicates a normally distributed profile and $S_{ku} > 3$ indicates a spiked profile. Spatial parameters reported are texture aspect ratio, S_{tr} and texture direction, S_{td}. Texture aspect ratio measures the directionality of the surface features. S_{tr} values close to zero indicate surface with a dominant directionality while values close to one indicate isotropic surfaces. Surface texture direction, S_{td}, measures the lay of the surface features.

Selected surface parameter values for the generated textured surfaces are detailed in Table 3. As can be seen from the table, the surface roughness (S_q) for the textured samples is 100 times higher than the polished samples. The skewness parameter, S_{sk}, shows that the textured samples have negative values suggesting that the bulk of the material is above the mean line. In contrast, the polished sample has a positive skewness. Main differences between the textures can be observed in the texture direction, S_{td}, and the texture aspect ratio, S_{tr}. The S_{tr} value for T1 was close to 1 indicating a nearly isotropic surface. This was expected given the laser scanning path used to achieve the pattern. On the other hand, S_{tr} for T3 was close to 0 indicating an anisotropic surface. Again, this was expected given the single-direction laser scanning path employed in processing the surface. The polished sample showed a texture direction, S_{td}, of 133°, which is due to the grinding marks left after polishing. In comparison to the textured samples, the texture direction for the polished sample can be disregarded given the significantly low roughness parameters. In other words, the polished sample can be considered to have flat isotropic surface.

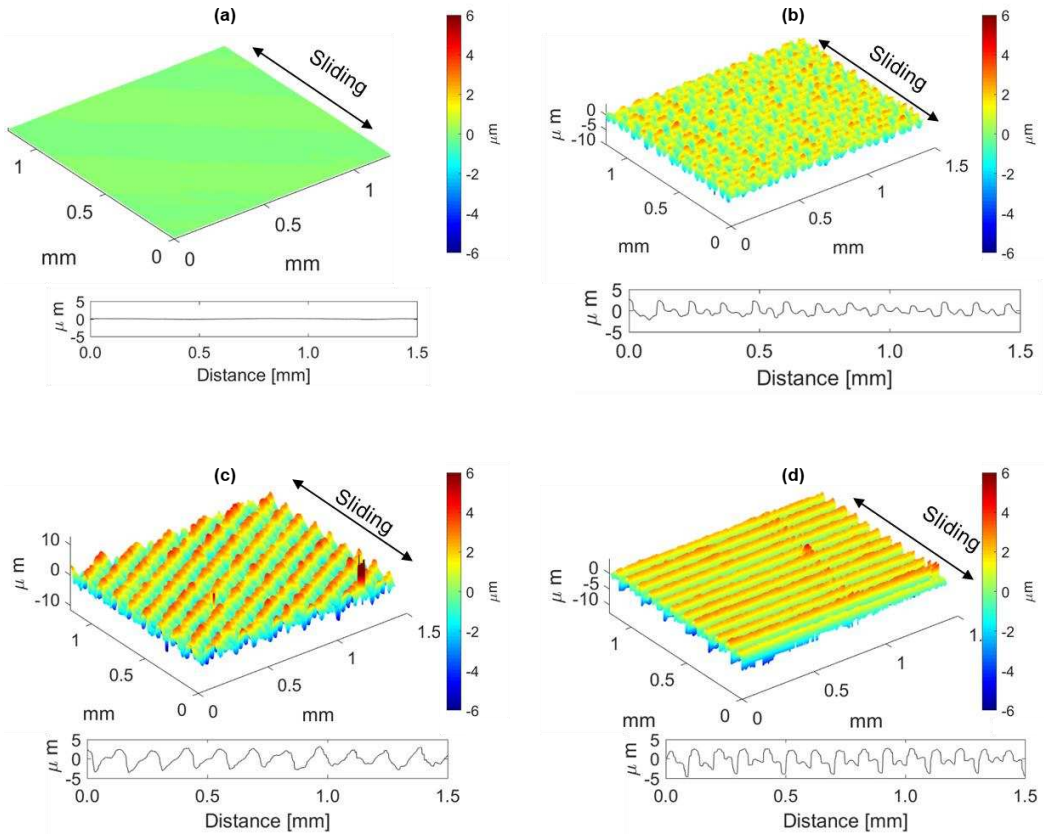

Figure 1. 3D images of the tested samples (a) polished (b) T1 (c) T2 (d) T3. Profiles were obtained along the sliding direction as indicated by the double arrow in each image.

Table 3. Surface parameters of steel surfaces

	Parameter	Polished	TI	T2	T3
Arithmetic mean height	S_a [µm]	0.007	0.791	0.766	0.922
Root mean square height	S_q [µm]	0.009	0.925	0.990	1.095
Skewness	S_{sk} [-]	0.441	-0.371	-0.821	-0.718
Kurtosis	S_{ku} [-]	3.048	2.128	3.535	2.687
Texture aspect ratio	S_{tr} [-]	0.034	0.835	0.619	0.016
Texture direction	S_{td} [°]	133	90	60	90

3.2 Friction performance

Figure 2(a) shows the friction curves during tests in BO. At the beginning of the tests, the friction coefficient was the same for polished, TI and T2 samples (µ=0.12). After rubbing for about 20 minutes, an increase in friction was observed in T1 and T2 samples reaching values above µ=0.14. The friction values for the polished and T3 samples remained unchanged throughout the duration of the test with the polished samples having lower friction than the T3 samples. In the absence of boundary additives, the applied textures in this study showed no friction performance improvement compared to polished samples.

Figure 2(b) shows the friction curves during tests with MoDTC. All the samples had initial friction coefficient values of 0.12. For T1 samples, the friction coefficient decreased slightly during the first few minutes of rubbing from an initial value of 0.12 to about 0.10 but then increased to reach values of about 0.14 at the end of the tests. With polished samples, the friction decreased rapidly after the test was initiated and reached steady values of 0.10 after 5 minutes of rubbing. In the case of T3 samples, the initial friction coefficient was maintained for about 30 minutes before friction reduction to steady

values of 0.09 was achieved. In previous studies, it has been shown that in tests with MoDTC additive, rapid friction reduction is observed after a short induction time. The length of the induction time is however dependent on various parameters such as the presence of other boundary additives and temperature [42]. In this study, it is evident that the surface topography also affects the induction period. A short induction time was observed for polished and T1 samples while a longer induction time was observed in T3 samples. The overall friction trend observed in polished and T3 samples, where an initial high friction drops to low values, is in agreement with previous studies [43].

Friction results from base oil and MoDTC tests are compared in Figure 2(c). It is clear that MoDTC resulted in friction reduction in polished, T2 and T3 samples.

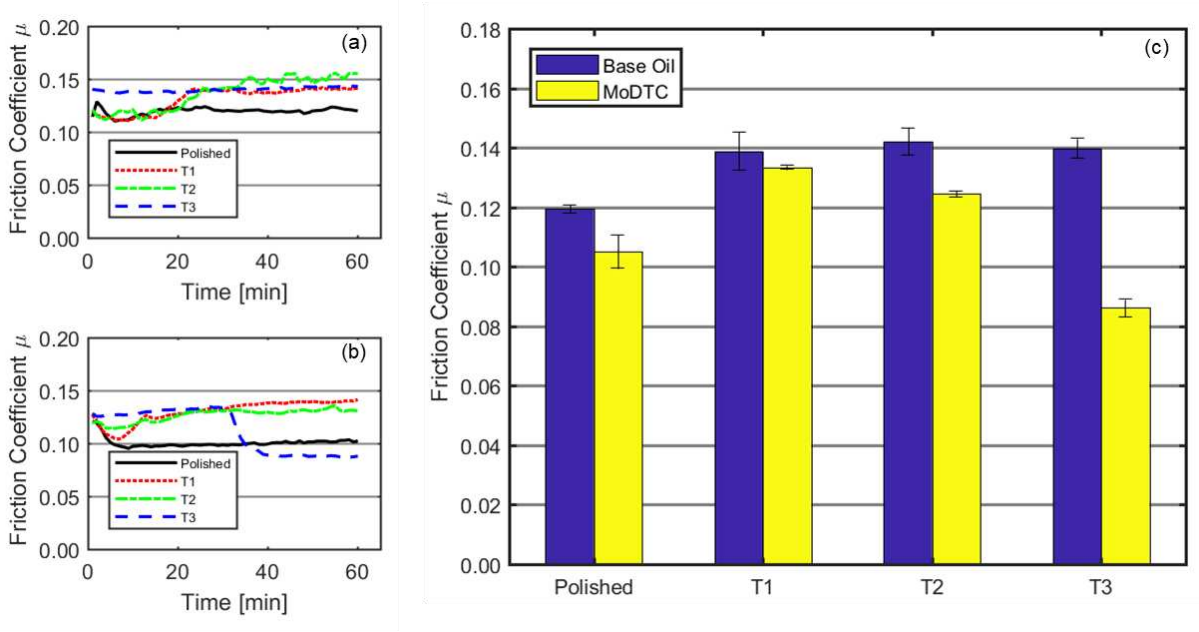

Figure 2. Friction curves during tests with (a) BO and (b) MoDTC. (c) Average friction during the last 20 minutes of the tests

3.3 Wear performance

Figure 3 shows contour plots of steel plates after tests with base oil and MoDTC highlighting the generated wear tracks. In tests with base oil, it can be observed that the features in all the textured samples were completely removed in the wear scars. In tests with MoDTC, some differences were observed in the generated wear scars with the various textures. With T1 samples, although the features were worn within the wear tracks, some of the texture features could still be observed. With T2 samples, the texture features were completely worn out in the wear track, similar to tests with base oil. In the case of T3 samples, the texture features were distinct within the wear track.

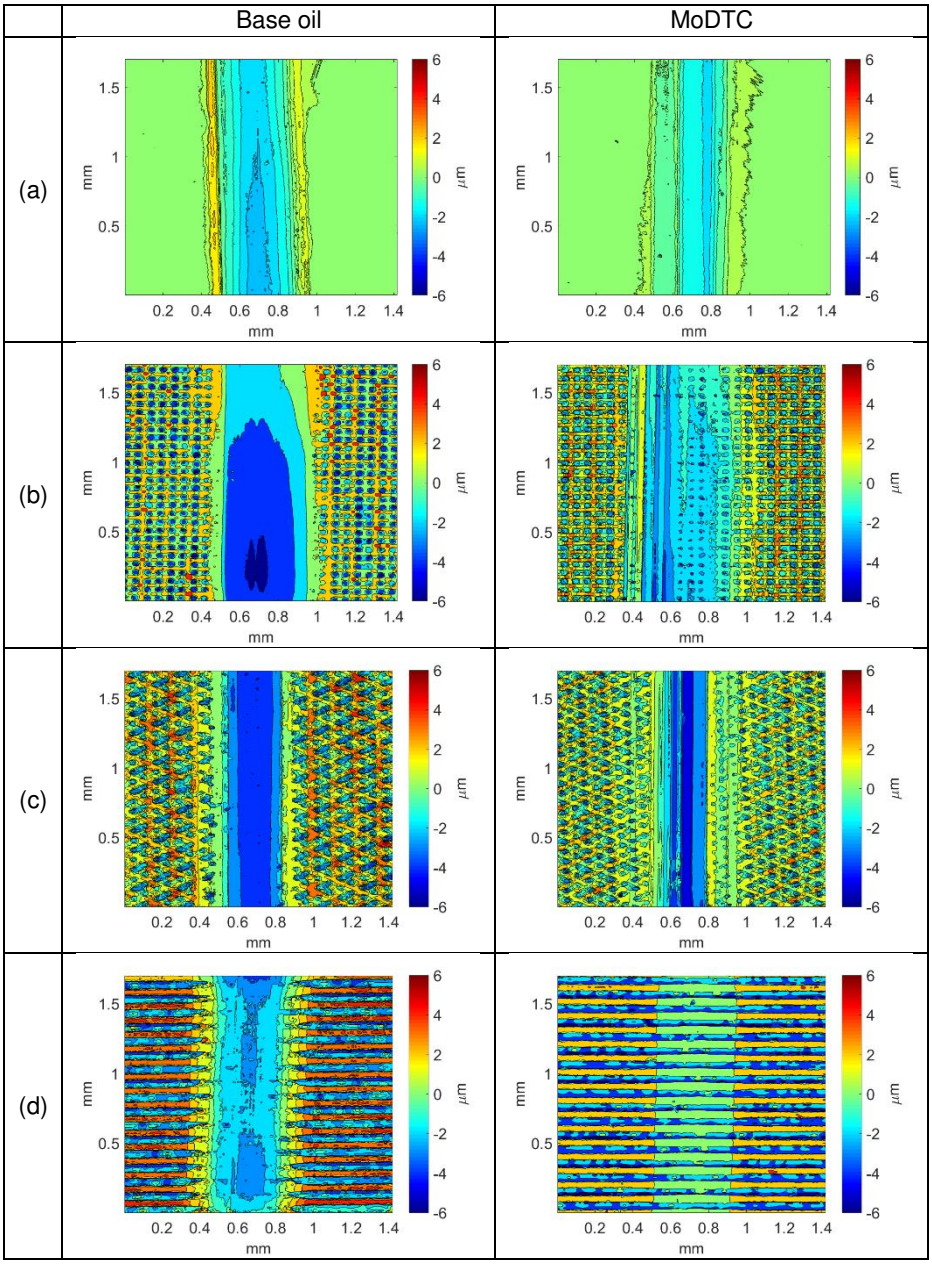

Figure 3. Contour plots of steel plates after tests with BO and MoDTC showing the generated wear scars. (a) Polished (b) T1 (c) T2 (d) T3.

Figure 4 shows profiles across wear scars for all the samples tested comparing wear depth in tests with BO and MoDTC. The profiles for T3 samples were obtained across the high regions of the topography. In all samples, it was observed that wear was improved in the presence of MoDTC in agreement with previous literature [44]. In polished samples, the maximum wear depth decreased from 2 µm in BO to 1.6 µm in MoDTC. In laser-processed samples, significant wear improvements with MoDTC were observed in T1 and T3 samples. In T1 sample, the maximum wear depth decreased from 5 µm in BO to 3 µm in MoDTC. In T3 sample, the maximum wear depth decreased from 5.7 µm in BO to 2.7 µm in MoDTC. Overall, these wear profiles show that higher wear was observed in textured samples compared to polished samples when both oils were used.

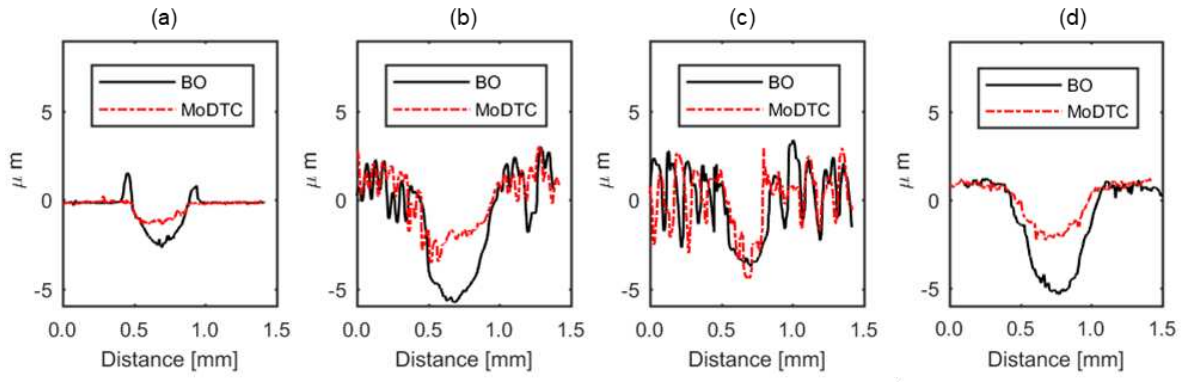

Figure 4. Profiles across the plate wear scars in tests with BO and MoDTC using (a) polished (b) T1 (c) T2 (d) T3 samples. The profiles were obtained from left to right of images in Figure 3

4 Discussion

4.1 Effect of textures in base oil

The BO contains no boundary additives, therefore friction and wear behaviour in these tests were influenced by the surface features and contact conditions. Results in this study showed that friction increased in all textured samples compared to polished samples in tests with base oil. The lower lambda ratio in textured samples compared to polished samples suggest a more severe contact. Simulation results presented in Part II of this study also indicate a more severe contact for textured samples compared to the polished samples. Thus, it is possible that the increased friction in textured samples was due to the severe contacts. It is however noted that the use of lambda ratio to depict contact severity is only applicable at the beginning of the tests as the surface roughness changes with rubbing. This is clearly seen in the surface topography images at the end of the tests (Figure 3) where the original textures have been smoothened resulting in a near polished surface for the textured samples.

Wear results showed that all the features from the laser-processed samples were removed from the surfaces at the end of the test. With the removal of the features, the surface topography of textured samples is similar to that of polished samples. As such, the textured samples would be expected to exhibit friction values similar to polished samples. This was however not the case as friction was still high at the end of the tests in the textured samples. Wear results showed that textured samples had deeper wear tracks than polished samples. The increased wear in textured samples would indicate a larger contact area between the counterparts. It is possible that the higher friction in textured samples could be attributed to the increased contact area. Furthermore, the higher wear in laser-processed samples could be attributed to third-body abrasive wear.

4.2 Effect of textures in oil with boundary additives

In tests with MoDTC, there was an overall wear performance improvement in all samples compared to tests with base oil. Improved wear performance in tests with MoDTC is expected if MoDTC additive decomposes to form a protective MoDTC tribofilm. These tribofilms, composed of molybdenum and sulphur provide both wear protection and friction reduction. Thus, in the absence of surface chemical analysis, friction reduction is a good indication for the formation of MoDTC tribofilms. Lower friction and wear depths in polished and T3 samples indicated the formation of MoDTC tribofilm in the samples. Although there was no rapid friction drop to low values in T1 and T2 samples, lower wear was observed suggesting the possibility for the formation of MoDTC tribofilms in the wear tracks.

The differences in friction and wear performance of the textures samples is better explained by the simulation results presented in Part II of this study. Simulations results revealed that of the three texture samples, T3 had better fluid entrainment into the contact at low speeds compared to the T1 and T2 samples. As such, the friction performance of T1 and T2 would be expected to be inferior to that of T3. This is because the formation of MoDTC tribofilms, responsible for friction reduction, is dependent on the availability of lubricant and sufficient shear in the contact for the additive decomposition. Despite the poor lubricant entrainment capabilities of textures T1 and T2, MoDTC tribofilms were somewhat formed which retarded the wear process. On the other hand, enhanced lubricant entrainment with T3 samples provided a constant supply of MoDTC additive for decomposition and tribofilm formation, hence the lower friction and wear values.

Compared to polished samples, T3 samples displayed a relatively long induction period before the friction drop to low values. To explain this observation, two simultaneous processes that occur within the contact have to be considered. These processes are tribofilm formation and removal. For a tribofilm to remain in the rubbing contact and friction drop to occur, the rate of tribofilm formation has to be greater than the rate of tribofilm removal.

The short induction period in polished samples suggests that the rate of tribofilm formation surpassed that of tribofilm formation during initial rubbing. From experimental calculations and simulation results (reported in Part II), it is evident that for polished samples, thicker lubricant films were entrained in the contact resulting in less severe contacts (initial mixed lubrication regime). Shearing of the lubricant films in polished samples caused additive decomposition resulting in tribofilm formation. The presence of a thicker lubricant film reduced the severity of the contact, which also inhibited or reduced tribofilm removal. Thus, the presence of thicker lubricant films in the polished samples could reasonably explain the shorter induction time.

On the other hand, the prolonged induction period in T3 samples suggest that the rates for tribofilm formation and removal were balanced during the initial rubbing period (30 minutes). From the initial calculations, T3 samples had much lower lambda ratios compared to polished samples, indicating that contacts were considerably severe in T3 samples. The entrained lubricant films in T3 samples enabled tribofilms to be formed. However, the severe contact caused the formed tribofilms to be removed at a similar rate as the formation rate. These contact conditions would explain the prolonged induction for the T3 samples. As there was no friction reduction during the first 30 minutes of rubbing, it is possible that the 2.7 µm wear observed in T3 samples occurred during this induction period. Wear during the induction period increased the contact area and subsequently increased the thickness of the entrained lubricant films. The reduced contact severity reduced the tribofilm removal rate resulting in the presence of stable tribofilms in the contact and friction drop to low values.

Lower friction observed in T3 samples compared to polished samples can be explained by the nature of tribofilms formed. Previous studies have shown that MoDTC decomposes to form tribofilms composed of various species, which in turn affect its friction performance [39,45]. Under ideal conditions, such as high temperature and high contact pressure, MoDTC is expected to decompose to form a tribofilm consisting of MoS_2 resulting in low friction coefficient values of about 0.04. However, in non-ideal conditions, such as low temperatures, MoDTC decomposes to form tribofilms composed of a mixture of MoS_2 and an amorphous compound consisting of molybdenum and sulphur (a-MoS_x) resulting in higher friction coefficient values (>0.04). Tests in this study were conducted at 40°C, which are non-ideal conditions, it is thus expected that the tribofilms formed would be composed of a mixture of a-MoS_x and crystalline MoS_2. The friction values obtained would decrease as the ratio of MoS_2/a-MoS_x increases in the tribofilms. It is thus possible that the difference in friction values for the polished and T3 samples is due to differences in the chemical composition of the formed tribofilms. Detailed chemical analysis of the resulting tribofilms will be conducted in future work. Nonetheless, the lower friction values with T3 samples compared to polished samples suggest that additive degradation can be enhanced through engineered surface topographies.

4.3 Effect of surface topography

From the results obtained in this present study, it is evident that surface topography plays a significant role in tribological performance in boundary lubrication regime. To elucidate the particular influence of the surface topography, an evaluation of various parameters and their relationship to friction was conducted.

Spatial parameters, texture direction, S_{td}, and texture aspect ratio, S_{tr}, of the surfaces were considered. The values for these spatial parameters were indicated earlier in Table 3. Although T1 and T3 exhibited similar feature alignment (same texture direction, S_{td}, value), differences were observed in the texture aspect ratio, S_{tr}. T1 is nearly isotropic while T3 is an anisotropic surface. Therefore, in correlating friction performance to spatial parameters, it was considered more logical to employ S_{tr} since it differentiates the different textures better. The correlation between friction coefficient and S_{tr} is shown in Figure 5. In tests with base oil, no correlation was observed with texture aspect ratio since the friction values were similar for all samples. However, in tests with MoDTC, a correlation was observed. These results suggest that an anisotropic surface can enhance the performance of the friction modifier used in this study when sliding perpendicular to the main features. This conclusion is in agreement with that obtained by Cousseau et al., [40] who reported friction improvement for MoDTC when sliding perpendicular to grinding marks while no friction improvement was observed when sliding parallel to the same grinding marks. It is however noted that for other boundary additives such as antiwear additives, other surface parameters may be more relevant. For example, Hsu et al., [46] reported that a surface with a texture pattern similar to T1 (isotropic surface) showed improved wear performance compared to an untextured sample in tests conducted with antiwear additive zinc dialkyldithiocarbamate (ZDDP). It is thus likely that in order to improve tribological performance of formulated oils containing antiwear additives and friction modifiers, surfaces topographies with optimised parameters will be essential.

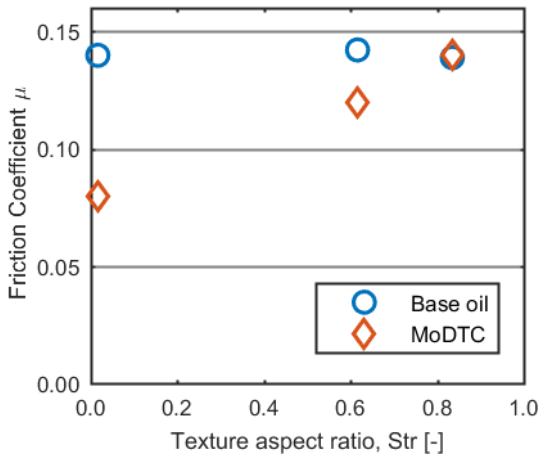

Figure 5. Relationship between friction coefficient and texture aspect ratio.

Besides, spatial parameters, other parameters were interrogated but no correlation to friction values was observed. It is worth mentioning that height parameters such as S_q are not adequate in describing the functionality of a surface with regard to boundary additives. If the surface functionality was dependent on the S_q value, all the textured samples would exhibit improved friction performance in line with previous studies where the distinguishing parameter was the S_q values [39,40]. It is thus concluded that a combination of spatial and height parameters is important in texture design for the tribological performance of the friction modifier tested. In future work, texture design optimisation will be conducted to improve tribological performance in fully formulated oils.

5 Conclusions

In this study, laser surface texturing using a nanosecond laser was employed to fabricate three different micro-scale features on steel surfaces. The friction performance of these textured samples was then investigated through tribological tests using base oil and model oil containing a boundary additive (MoDTC) in base oil. Results show that surface topographies dominated by micro-sized asperities have no beneficial impact on friction and wear compared to polished samples in tests conducted with base oil. Interestingly, in tests with model oil, anisotropic surfaces consisting of grooves-like features promoted additive degradation resulting in significant friction improvement. Although the best performing surface texture did not exhibit better wear performance compared to the untextured surface, it is envisioned that wear improvement can be achieved with texture design optimisation and the use of antiwear additives. This study has demonstrated that through careful selection of surface features, laser surface texturing can be successfully employed to improve the performance of additives in boundary lubrication regime.

References

[1] Holmberg K, Erdemir A. Influence of tribology on global energy consumption, costs and emissions. Friction 2017;5:263–84. https://doi.org/10.1007/s40544-017-0183-5.

[2] Devlin M. Common Properties of Lubricants that Affect Vehicle Fuel Efficiency: A North American Historical Perspective. Lubricants 2018;6:68. https://doi.org/10.3390/lubricants6030068.

[3] Niste VB, Tanaka H, Sugimura J. The Importance of Temperature in Generating ZDDP Tribofilms Efficient at Preventing Hydrogen Permeation in Rolling Contacts. Tribol Trans 2018;61:930–7. https://doi.org/10.1080/10402004.2018.1447180.

[4] Unnikrishnan R, Jain MC, Harinarayan AK, Mehta AK. Additive-additive interaction: An XPS study of the effect of ZDDP on the AW/EP characteristic of molybdenum based additives. Wear 2002;252:240–9. https://doi.org/10.1016/S0043-1648(01)00865-1.

[5] Fujita H, Spikes HA. Study of zinc dialkyldithiophosphate antiwear film formation and removal processes, part II: Kinetic model. Tribol Trans 2005;48:567–75. https://doi.org/10.1080/05698190500385187.

[6] Naveira-Suarez A, Tomala A, Grahn M, Zaccheddu M, Pasaribu R, Larsson R. The influence of base oil polarity and slide–roll ratio on additive-derived reaction layer formation. Proc Inst Mech Eng Part J J Eng Tribol 2011;225:565–76. https://doi.org/10.1177/1350650111405115.

[7] Rossi A, Eglin M, Piras FM, Matsumoto K, Spencer ND. Surface analytical studies of surface-additive interactions, by means of in situ and combinatorial approaches. Wear 2004;256:578–84. https://doi.org/10.1016/j.wear.2003.10.001.

[8] Yin Z, Kasrai M, Bancroft GM, Fyfe K, Colaianni ML, Tan KH. Application of soft X-ray absorption spectroscopy in chemical characterization of antiwear films generated by ZDDP Part II: The effect of detergents and dispersants. Wear 1997;202:192–201. https://doi.org/10.1016/S0043-1648(96)07273-0.

[9] Choa SH, Ludema KC, Potter GE, Dekoven BM, Morgan TA, Kar KK. A model of the dynamics of boundary film formation. Wear 1994;177:33–45. https://doi.org/10.1016/0043-1648(94)90115-5.

[10] Yin Z, Kasrai M, Fuller M, Bancroft GM, Fyfe K, Tan KH. Application of soft X-ray absorption spectroscopy in chemical characterization of antiwear films generated by ZDDP Part I: The effects of physical parameters. Wear 1997;202:172–91. https://doi.org/10.1016/S0043-1648(96)07272-9.

[11] Sugihara T, Enomoto T. Performance of cutting tools with dimple textured surfaces: A comparative study of different texture patterns. Precis Eng 2017;49:52–60. https://doi.org/10.1016/j.precisioneng.2017.01.009.

[12] Etsion I, Sher E. Improving fuel efficiency with laser surface textured piston rings. Tribol Int 2009;42:542–7. https://doi.org/10.1016/j.triboint.2008.02.015.

[13] Geiger M, Popp U, Engel U. Excimer laser micro texturing of cold forging tool surfaces - Influence on tool life. CIRP Ann - Manuf Technol 2002;51:231–4. https://doi.org/10.1016/S0007-8506(07)61506-6.

[14] Etsion I, Halperin G. A laser surface textured hydrostatic mechanical seal. Tribol Trans 2002;45:430–4. https://doi.org/10.1080/10402000208982570.

[15] Yu H, Wang X, Zhou F. Geometric shape effects of surface texture on the generation of hydrodynamic pressure between conformal contacting surfaces. Tribol Lett 2010;37:123–30. https://doi.org/10.1007/s11249-009-9497-4.

[16] Bouassida H, Biboulet N, Sainsot P, Lubrecht A. Piston ring load carrying capacity: Influence of cross-hatching parameters. Proc Inst Mech Eng Part J J Eng Tribol 2014;228:642–8. https://doi.org/10.1177/1350650114522779.

[17] Scaraggi M, Mezzapesa FP, Carbone G, Ancona A, Tricarico L. Friction properties of lubricated laser-microtextured-surfaces: An experimental study from boundary- to hydrodynamic-lubrication. Tribol Lett 2013;49:117–25. https://doi.org/10.1007/s11249-012-0045-2.

[18] Fowell M, Olver A V., Gosman AD, Spikes HA, Pegg I. Entrainment and inlet suction: Two mechanisms of hydrodynamic lubrication in textured bearings. J Tribol 2007;129:336–47. https://doi.org/10.1115/1.2540089.

[19] Wang WZ, Huang Z, Shen D, Kong L, Li S. The effect of triangle-shaped surface textures on the performance of the lubricated point-contacts. J Tribol 2013;135. https://doi.org/10.1115/1.4023206.

[20] Braun D, Greiner C, Schneider J, Gumbsch P. Efficiency of laser surface texturing in the reduction of friction under mixed lubrication. Tribol Int 2014;77:142–7. https://doi.org/10.1016/j.triboint.2014.04.012.

[21] Yuan S, Huang W, Wang X. Orientation effects of micro-grooves on sliding surfaces. Tribol Int 2011;44:1047–54. https://doi.org/10.1016/j.triboint.2011.04.007.

[22] Pettersson U, Jacobson S. Friction and wear properties of micro textured DLC coated surfaces in boundary lubricated sliding. Tribol Lett 2004;17:553–9. https://doi.org/10.1023/B:TRIL.0000044504.76164.4e.

[23] Varenberg M, Varenberg M, Halperin G, Etsion I. Different Aspects of the Role of Wear Debris in Fretting Wear. WEAR 2002:902--910.

[24] Zum Gahr KH, Mathieu M, Brylka B. Friction control by surface engineering of ceramic sliding pairs in water. Wear 2007;263:920–9. https://doi.org/10.1016/j.wear.2006.11.024.

[25] Wang L. Use of structured surfaces for friction and wear control on bearing surfaces. Surf Topogr Metrol Prop 2014;2. https://doi.org/10.1088/2051-672X/2/4/043001.

[26] Chiu YP. An analysis and prediction of lubricant film starvation in rolling contact systems. ASLE Trans 1974;17:22–35. https://doi.org/10.1080/05698197408981435.

[27] Blatter A, Maillat M, Pimenov SM, Shafeev GA, Simakin A V., Loubnin EN. Lubricated sliding performance of laser-patterned sapphire. Wear 1999;232:226–30. https://doi.org/10.1016/S0043-1648(99)00150-7.

[28] Demirci I, Mezghani S, Yousfi M, Zahouani H, Mansori M El. The Scale Effect of Roughness on Hydrodynamic Contact Friction. Tribol Trans 2012;55:705–12. https://doi.org/10.1080/10402004.2012.694990.

[29] Křupka I, Vrbka M, Hartl M. Effect of surface texturing on mixed lubricated non-conformal contacts. Tribol Int 2008;41:1063–73. https://doi.org/10.1016/j.triboint.2007.11.016.

[30] Vlădescu SC, Ciniero A, Tufail K, Gangopadhyay A, Reddyhoff T. Optimization of Pocket Geometry for Friction Reduction in Piston–Liner Contacts. Tribol Trans 2018;61:522–31. https://doi.org/10.1080/10402004.2017.1363930.

[31] Vlădescu SC, Olver A V., Pegg IG, Reddyhoff T. Combined friction and wear reduction in a reciprocating contact through laser surface texturing. Wear 2016;358–359:51–61. https://doi.org/10.1016/j.wear.2016.03.035.

[32] Vlədescu SC, Medina S, Olver A V., Pegg IG, Reddyhoff T. Lubricant film thickness and friction force measurements in a laser surface textured reciprocating line contact simulating the piston ring-liner pairing. Tribol Int 2016;98:317–29. https://doi.org/10.1016/j.triboint.2016.02.026.

[33] Vladescu SC, Olver A V., Pegg IG, Reddyhoff T. The effects of surface texture in reciprocating contacts

- An experimental study. Tribol Int 2015;82:28–42. https://doi.org/10.1016/j.triboint.2014.09.015.

[34] Vlădescu SC, Ciniero A, Tufail K, Gangopadhyay A, Reddyhoff T. Looking into a laser textured piston ring-liner contact. Tribol Int 2017;115:140–53. https://doi.org/10.1016/j.triboint.2017.04.051.

[35] Vlădescu SC, Medina S, Olver A V., Pegg IG, Reddyhoff T. The Transient Friction Response of a Laser-Textured, Reciprocating Contact to the Entrainment of Individual Pockets. Tribol Lett 2016;62. https://doi.org/10.1007/s11249-016-0669-8.

[36] Bonse J, Koter R, Hartelt M, Spaltmann D, Pentzien S, Höhm S, et al. Tribological performance of femtosecond laser-induced periodic surface structures on titanium and a high toughness bearing steel. Appl. Surf. Sci., vol. 336, Elsevier B.V.; 2015, p. 21–7. https://doi.org/10.1016/j.apsusc.2014.08.111.

[37] Bonse J, Koter R, Hartelt M, Spaltmann D, Pentzien S, Höhm S, et al. Femtosecond laser-induced periodic surface structures on steel and titanium alloy for tribological applications. Appl Phys A Mater Sci Process 2014;117:103–10. https://doi.org/10.1007/s00339-014-8229-2.

[38] Bettscheider S, Grützmacher P, Rosenkranz A. Low Friction and High Solid-Solid Contact Ratio—A Contradiction for Laser-Patterned Surfaces? Lubricants 2017;5:35. https://doi.org/10.3390/lubricants5030035.

[39] Khaemba DN, Jarnias F, Thiebaut B, Neville A, Morina A. The role of surface roughness and slide-roll ratio on the decomposition of MoDTC in tribological contacts. J Phys D Appl Phys 2017;50. https://doi.org/10.1088/1361-6463/aa5905.

[40] Cousseau T, Ruiz Acero JS, Sinatora A. Tribological response of fresh and used engine oils: The effect of surface texturing, roughness and fuel type. Tribol Int 2016;100:60–9. https://doi.org/10.1016/j.triboint.2015.11.016.

[41] Khaemba DN, Neville A, Morina A. New insights on the decomposition mechanism of Molybdenum DialkyldiThioCarbamate (MoDTC): A Raman spectroscopic study. RSC Adv 2016;6:38637–46. https://doi.org/10.1039/c6ra00652c.

[42] Morina A, Neville A, Priest M, Green JH. ZDDP and MoDTC interactions and their effect on tribological performance - Tribofilm characteristics and its evolution. Tribol Lett 2006;24:243–56. https://doi.org/10.1007/s11249-006-9123-7.

[43] Morina A, Neville A. Tribofilms: Aspects of formation, stability and removal. J Phys D Appl Phys 2007;40:5476–87. https://doi.org/10.1088/0022-3727/40/18/S08.

[44] Morina A, Neville A, Priest M, Green JH. ZDDP and MoDTC interactions in boundary lubrication-The effect of temperature and ZDDP/MoDTC ratio. Tribol Int 2006;39:1545–57. https://doi.org/10.1016/j.triboint.2006.03.001.

[45] Oumahi C, De Barros-Bouchet MI, Le Mogne T, Charrin C, Loridant S, Geantet C, et al. MoS 2 formation induced by amorphous MoS 3 species under lubricated friction. RSC Adv 2018;8:25867–72. https://doi.org/10.1039/c8ra03317j.

[46] Hsu C-J, Stratmann A, Rosenkranz A, Gachot C. Enhanced Growth of ZDDP-Based Tribofilms on Laser-Interference Patterned Cylinder Roller Bearings. Lubricants 2017;5:39. https://doi.org/10.3390/lubricants5040039.